

NUCLEOSYNTHETIC TUNGSTEN ISOTOPE ANOMALIES IN ACID LEACHATES OF THE MURCHISON CHONDRITE: IMPLICATIONS FOR HAFNIUM–TUNGSTEN CHRONOMETRY

CHRISTOPH BURKHARDT¹, THORSTEN KLEINE², NICOLAS DAUPHAS³, AND RAINER WIELER¹

¹ Institute of Geochemistry and Petrology, Clausiusstrasse 25, ETH Zurich, CH-8092 Zurich, Switzerland; burkhardt@erdw.ethz.ch

² Institut für Planetologie, Westfälische Wilhelms-Universität Münster, Wilhelm-Klemm-Strasse 10, D-48149 Münster, Germany

³ Origins Laboratory, Department of the Geophysical Sciences and Enrico Fermi Institute, The University of Chicago, 5734 South Ellis Avenue, Chicago, IL 60637, USA

Received 2012 March 30; accepted 2012 May 16; published 2012 June 13

ABSTRACT

Progressive dissolution of the Murchison carbonaceous chondrite with acids of increasing strengths reveals large internal W isotope variations that reflect a heterogeneous distribution of *s*- and *r*-process W isotopes among the components of primitive chondrites. At least two distinct carriers of nucleosynthetic W isotope anomalies must be present, which were produced in different nucleosynthetic environments. The co-variation of $^{182}\text{W}/^{184}\text{W}$ and $^{183}\text{W}/^{184}\text{W}$ in the leachates follows a linear trend that is consistent with a mixing line between terrestrial W and a presumed *s*-process-enriched component. The composition of the *s*-enriched component agrees reasonably well with that predicted by the stellar model of *s*-process nucleosynthesis. The co-variation of $^{182}\text{W}/^{184}\text{W}$ and $^{183}\text{W}/^{184}\text{W}$ in the leachates provides a means for correcting the measured $^{182}\text{W}/^{184}\text{W}$ and $^{182}\text{W}/^{183}\text{W}$ of Ca–Al-rich inclusions (CAI) for nucleosynthetic anomalies using the isotopic variations in $^{183}\text{W}/^{184}\text{W}$. This new correction procedure is different from that used previously, and results in a downward shift of the initial $\varepsilon^{182}\text{W}$ of CAI to -3.51 ± 0.10 (where $\varepsilon^{182}\text{W}$ is the variation in 0.01% of the $^{182}\text{W}/^{183}\text{W}$ ratio relative to Earth’s mantle). This revision leads to Hf–W model ages of core formation in iron meteorite parent bodies that are ~ 2 Myr younger than previously calculated. The revised Hf–W model ages are consistent with CAI being the oldest solids formed in the solar system, and indicate that core formation in some planetesimals occurred within ~ 2 Myr of the beginning of the solar system.

Key words: meteorites, meteors, meteoroids – minor planets, asteroids: general – nuclear reactions, nucleosynthesis, abundances – stars: AGB and post-AGB

1. INTRODUCTION

The decay of the now extinct ^{182}Hf to ^{182}W ($t_{1/2} \approx 8.9$ Myr) is a powerful tool to study the timescales of planetary accretion and core formation (Jacobsen 2005; Kleine et al. 2009). The fact that both Hf and W are refractory and have very different geochemical behavior during metal–silicate separation renders this chronometer uniquely useful to study the timing of metal segregation (Lee & Halliday 1995; Harper & Jacobsen 1996). Accurate application of Hf–W chronometry requires knowledge of the present-day W isotopic composition of chondrites (i.e., undifferentiated meteorites thought to represent the composition of bulk planetary bodies for refractory elements; Kleine et al. 2002; Schoenberg et al. 2002; Yin et al. 2002), and of the initial $^{182}\text{Hf}/^{180}\text{Hf}$ and $^{182}\text{W}/^{184}\text{W}$ ratios at the beginning of the solar system. The latter two parameters can be constrained by investigating the Hf–W systematics of Ca–Al-rich inclusions (CAI; Burkhardt et al. 2008), which are generally considered to be the first solid material formed within the solar nebula (Grossman 1972) ~ 4.567 billion years ago (Amelin et al. 2010; Bouvier & Wadhwa 2010).

Accurate and precise knowledge of the initial $^{182}\text{W}/^{184}\text{W}$ of the solar system is particularly important for applying the Hf–W system to date metal segregation in the parent bodies of magmatic iron meteorites. These are considered to sample the metal cores of small planetary bodies (Scott & Wasson 1975). During metal segregation, Hf is retained in the silicate mantle, while W preferentially partitions into the metal core. Because the core has $\text{Hf}/\text{W} \approx 0$, it maintains the $^{182}\text{W}/^{184}\text{W}$ acquired at the time of core formation. Precise Hf–W ages of

metal segregation can be calculated, therefore, by comparing the $^{182}\text{W}/^{184}\text{W}$ of iron meteorites to the initial value (before ^{182}Hf -decay) determined for CAI (Kleine et al. 2005).

As is evident from strong ^{182}W deficits in magmatic iron meteorites, core formation in their parent bodies was a very early process (Kleine et al. 2005; Markowski et al. 2006a, 2006b; Scherstén et al. 2006; Qin et al. 2008a). Surprisingly, however, most iron meteorites exhibit $^{182}\text{W}/^{184}\text{W}$ lower than the solar system initial. This may in part reflect the effects of neutron-capture reactions on W isotopes induced during cosmic-ray exposure (Leya et al. 2003; Masarik 1997), but even after correction of these effects many iron meteorites still have $^{182}\text{W}/^{184}\text{W}$ ratios close to or even below the CAI initial.

The interpretation of the W isotope data for iron meteorites critically depends on the accuracy of the initial $^{182}\text{W}/^{184}\text{W}$ at the beginning of the solar system as inferred from CAI. The initial $^{182}\text{W}/^{184}\text{W}$ of CAI might be too high as a result of mobilization and re-distribution of radiogenic W during parent body alteration (Humayun et al. 2007), but the Hf–W systematics of CAI do not show evidence for such a re-distribution (Burkhardt et al. 2008).

A more severe problem might be nucleosynthetic isotope anomalies in CAI (Birck 2004; Wasserburg et al. 2011). Tungsten has five stable isotopes: the rare ^{180}W , a pure *p*-process nuclide, and ^{182}W , ^{183}W , ^{184}W , and ^{186}W , which are produced by both *s*- and the *r*-processes. A heterogeneous distribution of *p*-, *s*-, and *r*-process nuclides, therefore, will lead to variable relative abundances of the different W isotopes. Most CAI investigated so far show small nucleosynthetic W isotope anomalies (Burkhardt et al.

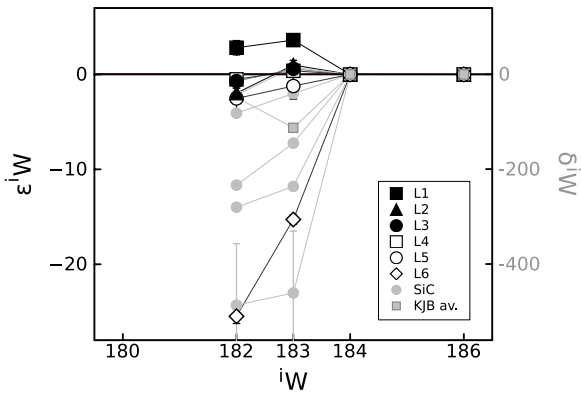


Figure 1. W isotopic data for Murchison leachates (this study), mainstream SiC grains, and the SiC-enriched KJB separate (Ávila et al. 2012) for normalization to $^{186}\text{W}/^{184}\text{W}$. To avoid overcrowding, error bars for SiC data are only shown for one grain.

2008), but how this affects the initial $^{182}\text{W}/^{184}\text{W}$ measured for CAI is currently unclear. Assessing the contribution of nucleosynthetic isotope anomalies to variations in ^{182}W requires knowledge of the relative effects on radiogenic (i.e., ^{182}W) and non-radiogenic W isotopes (i.e., ^{183}W , ^{184}W , ^{186}W). However, with the exception of W isotope measurements for presolar SiC grains (Ávila et al. 2012), such information is currently only available from theoretical models of stellar nucleosynthesis (e.g., Arlandini et al. 1999).

To better constrain the distinct nucleosynthetic W isotope components that were present in the solar nebula, we measured the isotopic composition of W released during the sequential dissolution of the primitive chondrite Murchison (CM2). The new W isotopic data provide an improved understanding of the stellar nucleosynthesis of W, which is critical for distinguishing between nucleosynthetic and radiogenic contributions to variations in ^{182}W . The new results require a downward revision of the initial $^{182}\text{W}/^{184}\text{W}$ of CAI and have important implications for the chronology of metal segregation in planetesimals.

2. TUNGSTEN ISOTOPE ANOMALIES IN MURCHISON

A powdered sample (≈ 16.5 g) of the Murchison carbonaceous chondrite was sequentially digested using acids of increasing strengths (see Reisberg et al. 2009). The insoluble residue (L6) left after acid treatment was fused with a CO_2 laser, to ensure complete dissolution of all remaining presolar grains (see Burkhardt et al. 2011). All samples were digested in acids (aqua regia for L1–L5; HNO_3 –HF– HClO_4 for L6) and W was purified from these samples by anion exchange chemistry in HCl–HF media (Kleine et al. 2004). All W isotope measurements were performed by multicollector inductively coupled plasma mass spectrometry at ETH Zurich. Aliquots of the same solutions were previously analyzed for Os and Mo isotopic compositions (Burkhardt et al. 2012; Reisberg et al. 2009).

The W isotope ratios are displayed in Table 1 and are reported in the $\epsilon^i\text{W}$ notation (i.e., part per 10,000 deviations from the terrestrial W isotopic composition). Instrumental mass bias was corrected by normalization to either $^{186}\text{W}/^{184}\text{W}$ or $^{186}\text{W}/^{183}\text{W}$. Since samples having nucleosynthetic W isotope anomalies have different $^{186}\text{W}/^{184}\text{W}$ and $^{186}\text{W}/^{183}\text{W}$, the mass bias correction results in different $\epsilon^{182}\text{W}$ for these two normalizations. A heterogeneous distribution of *s*- and *r*-process W isotopes affects ^{184}W more strongly than other W isotopes, because ^{184}W has the largest *s*-process contribution of all W

isotopes. Any nucleosynthetic anomalies are therefore larger for $^{181}\text{W}/^{184}\text{W}$ (normalized to $^{186}\text{W}/^{184}\text{W}$) than they are for $^{181}\text{W}/^{183}\text{W}$ (normalized to $^{186}\text{W}/^{183}\text{W}$). The former normalization, therefore, is best suited for constraining the *s*-process nucleosynthesis of W isotopes and, hence, for assessing the effects of nucleosynthetic anomalies on ^{182}Hf – ^{182}W chronometry. In contrast, normalization to $^{186}\text{W}/^{183}\text{W}$ is best suited for correcting measured $\epsilon^{182}\text{W}$ values for nucleosynthetic anomalies, because the nucleosynthetic effects on $\epsilon^{182}\text{W}$ are small for this normalization.

The leaching experiment reveals large internal W isotopic variations, indicating that Murchison contains material produced in distinct nucleosynthetic settings. Figure 1 shows the W isotope data in an $\epsilon^i\text{W}$ – $i\text{W}$ plot and reveals that the W isotope patterns of the leachates are similar, albeit of much smaller magnitude, than those measured for SiC grains from the Murchison chondrite (Ávila et al. 2012). The $\epsilon^{183}\text{W}$ values of the leachates decrease from +3.6 for L1 (acetic acid leachate) to –15.3 for L6 (insoluble residue), while at the same time the $\epsilon^{182}\text{W}$ values decrease from +2.8 (L1) to –25.5 (L6). This results in a positive correlation between $\epsilon^{183}\text{W}$ and $\epsilon^{182}\text{W}$ (Figure 2). The weighted average of the W isotopic compositions of the leachates agrees with the bulk measurement (e.g., Kleine et al. 2004), indicating that all important nucleosynthetic W isotope components have been tapped by the leaching experiment.

3. NATURE AND ORIGIN OF W ISOTOPIC ANOMALIES

A deficit in *s*-process W isotopes will lead to a higher-than-terrestrial $^{183}\text{W}/^{184}\text{W}$ (i.e., positive $\epsilon^{183}\text{W}$), because ^{184}W has a larger *s*-process contribution than the other W isotopes. Thus, the leachates L1–3, which all have positive $\epsilon^{183}\text{W}$, show an *s*-deficit (or *r*-excess), whereas the negative $\epsilon^{183}\text{W}$ of leachates L5 and L6 indicate an *s*-excess (*r*-deficit) in these samples. A distinction between an *s*-deficit and an *r*-excess would require ^{180}W data, but the low W contents in the individual leach steps did not permit reliable ^{180}W measurements.

The $\epsilon^{182}\text{W}$ – $\epsilon^{183}\text{W}$ correlation defined by the leachate data is in reasonable agreement with predictions of the stellar model of *s*-process nucleosynthesis (Arlandini et al. 1999), but has a slightly shallower slope than that predicted by this model (Figure 2(a)). After correction of measured $\epsilon^{182}\text{W}$ values for ^{182}Hf -decay using their measured $^{180}\text{Hf}/^{184}\text{W}$ and the initial $^{182}\text{Hf}/^{180}\text{Hf}$ of CAI (Burkhardt et al. 2008), the slope of the $\epsilon^{182}\text{W}_i$ – $\epsilon^{183}\text{W}$ correlation becomes slightly steeper than that obtained from the stellar model (Figure 2(b)). It remains unclear, however, if this steeper slope provides a closer match to the true *s*-process contribution to the different W isotopes, because the decay correction of the measured $\epsilon^{182}\text{W}$ values may be inaccurate due to heterogeneities in $^{182}\text{Hf}/^{180}\text{Hf}$ and/or incongruent dissolution of Hf and W during leaching. Nevertheless, overall the W isotope data agree quite well with the predictions of the stellar *s*-process model.

As expected for samples having nucleosynthetic W isotopic anomalies, the leachate data do not plot on an isochron (Figure 3, gray symbols). After correction for nucleosynthetic ^{182}W anomalies using the anomalies in $\epsilon^{183}\text{W}$ and the $\epsilon^{182}\text{W}$ – $\epsilon^{183}\text{W}$ correlation of Arlandini et al. (1999), still no isochronous relationship is obtained (Figure 3, bold symbols).

The remaining scatter of the Hf–W data around the CAI isochron could be due to ^{182}Hf heterogeneities in the diverse Murchison components, because the maximum departure from the isochron ($\approx -3.6 \epsilon^{182}\text{W}$) corresponds approximately to the initial solar system $\epsilon^{182}\text{W}$ value ($\approx -3.5 \epsilon^{182}\text{W}$ with

Table 1
Hf–W Data for Acid Leachates of Murchison and Allende CAI

Sample	N	Hf [ng/g]	W [ng/g]	$^{180}\text{Hf}/^{184}\text{W}$	$\epsilon^{182}\text{W}$	$\epsilon^{183}\text{W}$	$\epsilon^{182}\text{W}_i$	$\epsilon^{182}\text{W}_{s\text{-corrected}}$	$\epsilon^{182}\text{W}$	$\epsilon^{184}\text{W}$	$\epsilon^{182}\text{W}_i$	$\epsilon^{182}\text{W}_{s\text{-corrected}}$		
						Internally normalized to $^{186}\text{W}/^{184}\text{W} = 0.92767$				Internally normalized to $^{186}\text{W}/^{183}\text{W} = 1.98594$				
Murchison														
Leachate L1		9M HAc, 1 day, 20 °C	1	14.49 ± 0.04	7.83 ± 0.20	2.18 ± 0.06	2.81 ± 0.76	3.62 ± 0.50	0.36 ± 0.81	−3.29 ± 1.12	−2.09 ± 0.96	−2.40 ± 0.33	−4.56 ± 0.97	−3.35 ± 0.97
Leachate L2		4.7 M HNO ₃ , 5 days, 20 °C	1	30.70 ± 0.11	20.85 ± 0.36	1.74 ± 0.03	−1.97 ± 0.76	0.99 ± 0.50	−3.92 ± 0.79	−3.64 ± 1.12	−3.34 ± 0.96	−0.66 ± 0.33	−5.31 ± 0.97	−3.69 ± 0.97
Leachate L3		5.5M HCl, 1 day, 75 °C	1	10.48 ± 0.06	27.42 ± 0.39	0.45 ± 0.01	−0.70 ± 0.76	0.59 ± 0.50	−1.21 ± 0.76	−1.69 ± 1.12	−1.78 ± 0.96	−0.39 ± 0.33	−2.29 ± 0.96	−1.98 ± 0.97
Leachate L4		13M HF/3M HCl, 1 day, 75 °C	2	41.22 ± 0.14	59.43 ± 0.76	0.82 ± 0.01	−0.52 ± 0.36	0.38 ± 0.28	−1.44 ± 0.37	−1.16 ± 0.58	−0.94 ± 0.59	−0.25 ± 0.19	−1.87 ± 0.59	−1.07 ± 0.60
Leachate L5		13M HF/6M HCl, 3 day, 150 °C	1	8.47 ± 0.03	3.00 ± 0.20	3.33 ± 0.22	−2.53 ± 1.59	−1.22 ± 1.38	−6.28 ± 1.72	−0.47 ± 2.77	−0.91 ± 0.81	0.81 ± 0.92	−4.69 ± 0.87	−0.49 ± 0.91
Residue L6		Insoluble residue, Laser fused	1	23.73 ± 0.04	4.50 ± 0.23	6.22 ± 0.31	−25.48 ± 0.76	−15.28 ± 0.50	−32.47 ± 1.27	0.28 ± 1.12	−4.48 ± 0.96	10.18 ± 0.33	−11.53 ± 1.07	0.85 ± 0.97
Weighted average leachates				129.1 ± 0.2	123.0 ± 1.0	1.24 ± 0.01	−1.56 ± 0.59	0.12 ± 0.42	−2.95 ± 0.62	−1.77 ± 0.90	−1.74 ± 0.78	−0.08 ± 0.28	−3.14 ± 0.79	−1.78 ± 0.79
Bulk Murchison fused			1	149.0 ± 0.2	133.6 ± 0.3	1.32 ± 0.01	−2.13 ± 0.76	0.08 ± 0.50	−3.61 ± 0.77	−2.26 ± 1.11	−2.32 ± 0.96	−0.05 ± 0.33	−3.81 ± 0.96	−2.35 ± 0.97
Allende CAI														
A-ZH-1	Type B		4			1.83 ± 0.01	−1.23 ± 0.33	0.18 ± 0.47	−3.31 ± 0.33	−1.53 ± 0.86	−1.50 ± 0.52	−0.12 ± 0.31	−3.59 ± 0.52	−1.56 ± 0.54
A-ZH-2	Type B		6			2.02 ± 0.01	−0.80 ± 0.11	0.35 ± 0.09	−3.09 ± 0.11	−1.39 ± 0.22	−1.20 ± 0.13	−0.19 ± 0.08	−3.50 ± 0.13	−1.30 ± 0.13
A-ZH-4	Type B		2			2.12 ± 0.01	−0.55 ± 0.62	0.54 ± 0.35	−2.95 ± 0.62	−1.46 ± 0.88	−1.25 ± 0.30	−0.36 ± 0.23	−3.67 ± 0.30	−1.44 ± 0.33
A-ZH-5	Type A		3			1.79 ± 0.01	2.21 ± 0.20	2.57 ± 0.36	0.19 ± 0.25	−2.12 ± 1.08	−1.14 ± 0.38	−1.71 ± 0.24	−3.17 ± 0.47	−2.03 ± 0.44

Notes. *Leachates:* Hf and W concentrations were determined on small aliquots by isotope dilution using a ^{180}Hf – ^{183}W tracer. Blanks for the W isotope and Hf–W concentration measurements were negligible. The blank of the leaching procedure itself could not be assessed, but is small because only ultra-pure reagents were used (see Reisberg et al. 2009). W isotope measurements were made with ion beam intensities between 3×10^{-12} and 2.5×10^{-11} A on ^{184}W , and consisted of 60 s baseline measurements (made on-peak) followed by 40 isotope ratio measurements of 5 s each. Instrumental mass bias was corrected using the exponential law and $^{186}\text{W}/^{184}\text{W} = 0.92767$ or $^{186}\text{W}/^{183}\text{W} = 1.98594$. Isobaric Os interferences on ^{184}W and ^{186}W were corrected by monitoring ^{188}Os . Interference corrections ranged from 0.04 (L6) to 24.19 (L1) ϵ -units on $\epsilon^{182}\text{W}$ and from 0.02 to 11.92 ϵ -units on $\epsilon^{183}\text{W}$, respectively. W isotope ratios are reported as deviations from the terrestrial standard as follows: $\epsilon^i\text{W} = [(^{i}\text{W}/^{184}\text{W})_{\text{sample}} / (^{i}\text{W}/^{184}\text{W})_{\text{standard}} - 1] \times 10^4$. Uncertainties correspond to the reproducibility (2SD) of the W standards measured at the same concentration than the samples or the internal error, whichever is larger. *Allende CAI:* Data renormalized from Burkhardt et al. (2008). Uncertainties are 95% confidence intervals.

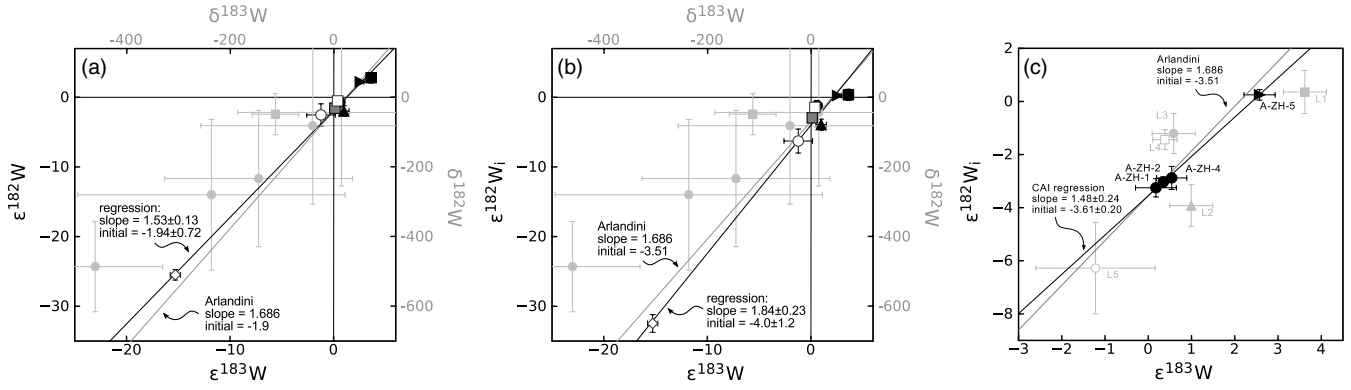


Figure 2. $\epsilon^{183}\text{W}$ vs. $\epsilon^{182}\text{W}$ and $\epsilon^{182}\text{W}_i$ plots for Murchison leachates (a) and (b) and CAI (c). Symbols are the same as in Figure 1, except in (c), where leachates are given in gray. Gray lines represent mixing lines between a theoretical s -process component (Arlandini et al. 1999) and average solar system W, black solid lines are regressions calculated for the measured (a) and decay-corrected (b) $\epsilon^{182}\text{W}$ values of the leachates, and for the decay-corrected $\epsilon^{182}\text{W}$ values of bulk CAI (c). All regressions were calculated using IsoPlot (Ludwig 1991).

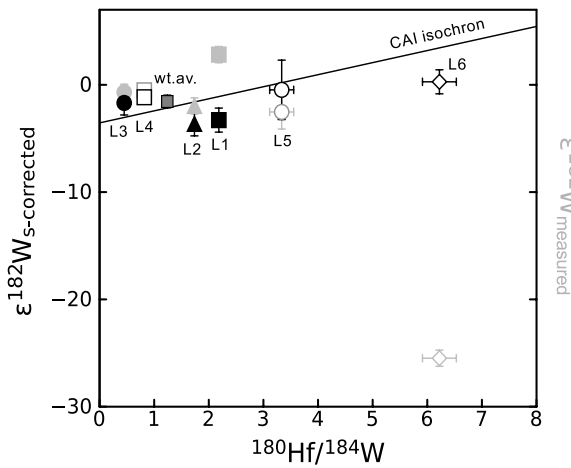


Figure 3. Hf–W isochron diagram for Murchison leachates. The measured data (light gray symbols) do not show an isochronous relationship. After correction for nucleosynthetic anomalies using $\epsilon^{182}\text{W}_{s\text{-corrected}} = \epsilon^{182}\text{W}_{\text{measured}}$ a better correlation is obtained, but the data still scatter around the CAI isochron.

$^{182}\text{Hf}/^{180}\text{Hf} \approx 1 \times 10^{-4}$). At large scales, the early solar system timescale given by the ^{182}Hf – ^{182}W system is in good agreement with other extinct and extant radiochronometers (Kleine et al. 2009, 2012; Nyquist et al. 2009), supporting a homogeneous distribution of ^{182}Hf . However, as to whether ^{182}Hf is heterogeneous at a finer scale such as that tapped by meteorite leachates is an open question and will require further work. The dispersion of the W isotope data in the Hf–W isochron diagram (Figure 3) may also be due to incongruent dissolution of Hf and W during leaching, leading to incorrect measured Hf/W ratios and, hence, inaccurate correction for ^{182}Hf -decay. Finally, the excess scatter on the $\epsilon^{182}\text{W}_i$ – $\epsilon^{183}\text{W}$ correlation line may also reflect the presence of different W carriers characterized by variable s -process compositions, because different thermal pulses and changing C/O ratios in AGB stars may have a substantial effect on the s -process yields of W isotopes (Ávila et al. 2012).

4. NUCLEOSYNTHETIC W ISOTOPE ANOMALIES IN CAI AND THE INITIAL W ISOTOPIC COMPOSITION OF THE SOLAR SYSTEM

The discussion up to this point highlights that phases with variable W isotopic compositions were present in the solar nebula and are preserved in primitive chondrites. A heterogeneous

distribution of these different phases would produce nucleosynthetic W isotopic anomalies, which may affect the use of the ^{182}Hf – ^{182}W system to infer the timescales of early solar system processes. However, with the exception of small ^{184}W deficits in IVB iron meteorites (Qin et al. 2008b) no nucleosynthetic W isotope anomalies have been identified at the bulk meteorite scale so far. The presence of distinct presolar carriers of nucleosynthetic W isotope anomalies, therefore, does not appear to affect the use of Hf–W chronometry to date bulk meteorites or events at the bulk planetary scale.

However, most of the CAI investigated so far show resolvable nucleosynthetic W isotope anomalies (Table 1; Burkhardt et al. 2008). The fine-grained type A CAI A-ZH-5 exhibits a nucleosynthetic W isotope anomaly of $\epsilon^{183}\text{W} = +2.57 \pm 0.36$, while type B CAI show much smaller anomalies averaging at $\epsilon^{183}\text{W} = +0.32 \pm 0.14$ (rel. $^{186}\text{W}/^{184}\text{W}$) or $\epsilon^{184}\text{W} = -0.20 \pm 0.09$ (rel. $^{186}\text{W}/^{183}\text{W}$). Previous studies had to rely on predictions of theoretical models for s -process nucleosynthesis to quantify the effects of nucleosynthetic anomalies on $\epsilon^{182}\text{W}$ (see Qin et al. 2008b). However, the s -process path in the Hf–Ta–W–Re–Os region of the nuclide chart is not well understood (e.g., Ávila et al. 2012), making such predictions uncertain. In contrast, the new W isotopic data presented here provide the first direct measurement of correlated nucleosynthetic effects on the different W isotopes, and as such provide a powerful means for quantifying nucleosynthetic anomalies on $\epsilon^{182}\text{W}$.

Qin et al. (2008b), using Maxwellian-averaged cross sections (MACS) from Bao et al. (2000), calculated that nucleosynthetic W isotope anomalies in $\epsilon^{182}\text{W}$ (rel. $^{186}\text{W}/^{183}\text{W}$) are 0.04 times those in $\epsilon^{184}\text{W}$. However, Qin et al. (2008b) also noted that the MACS of Bao et al. (2000) led to a predicted r -process ^{182}W residual abundance that was too high, and suggested that this overproduction problem may be resolved if the MACS value of ^{182}W was reduced by $\approx 20\%$. Using the modified value, a slope of ≈ 0.5 was obtained for the $\epsilon^{182}\text{W}$ – $\epsilon^{184}\text{W}$ correlation line. However, Burkhardt et al. (2008) found that the CAI A-ZH-5 plots above the ≈ 0.5 slope $\epsilon^{182}\text{W}$ – $\epsilon^{184}\text{W}$ correlation, but is consistent with the shallower slope obtained from the standard MACS of Bao et al. (2000). The average $\epsilon^{184}\text{W}$ anomaly of ≈ -0.2 observed for type B CAI would thus require a correction of only $+0.008$ $\epsilon^{182}\text{W}$ (using a slope of 0.04 for the $\epsilon^{182}\text{W}$ – $\epsilon^{184}\text{W}$ correlation), which is far smaller than the analytical uncertainty of the W isotope measurements. For this reason, Burkhardt et al. (2008) did not correct their W isotope data for nucleosynthetic anomalies and concluded

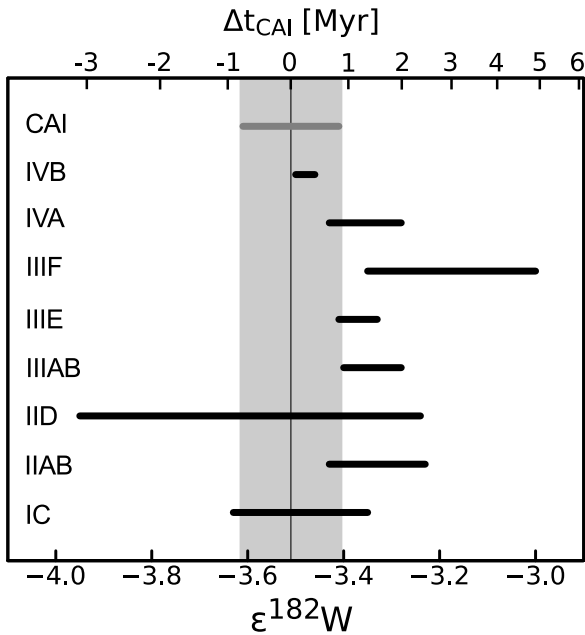


Figure 4. Hf–W model ages for core formation in iron meteorite parent bodies (W isotopic data from Qin et al. 2008a). The revised CAI initial of $\epsilon^{182}\text{W} = -3.51 \pm 0.10$ is lower than (albeit not resolvable from) $\epsilon^{182}\text{W}$ values for iron meteorites corrected for cosmic-ray-induced W isotope variations. This indicates that core formation in the parent bodies of magmatic iron meteorites occurred within ~ 2 Myr after CAI formation.

that (except for A-ZH-5) the small nucleosynthetic W isotope anomalies have no significant effects on the Hf–W systematics of CAI. However, the co-variation of $\epsilon^{182}\text{W}$ with anomalies in non-radiogenic W isotopes in the different leaching steps of Murchison presented here does not follow any of the two previously proposed correlation lines but is consistent with the predictions of the stellar model of Arlandini et al. (1999) (Figure 2). This requires re-assessing the significance of small nucleosynthetic W isotope anomalies for the Hf–W systematics of CAI.

In a plot of $(\epsilon^{182}\text{W})_i$ versus $\epsilon^{183}\text{W}$ (Figure 2(c)) the CAI plot along a straight line with a slope of 1.48 ± 0.24 , consistent with a slope of ≈ 1.686 predicted by the stellar model of Arlandini et al. (1999) for normalization to $^{186}\text{W}/^{184}\text{W}$. The different leach steps from Murchison also plot on or close to the correlation line defined by the CAI, indicating that the nucleosynthetic W isotope anomalies in the CAI and leachates have a common origin. A linear regression of the CAI data yields an $(\epsilon^{182}\text{W})_i$ value of -3.61 ± 0.20 at $\epsilon^{183}\text{W} = 0$, which provides the initial $\epsilon^{182}\text{W}$ of CAI corrected for nucleosynthetic effects. The same approach using the W isotope data normalized to $^{186}\text{W}/^{183}\text{W}$ yields an $(\epsilon^{182}\text{W})_i$ value of -3.57 ± 0.14 at $\epsilon^{184}\text{W} = 0$. Both normalizations, therefore, yield consistent initial $\epsilon^{182}\text{W}$ values after correction for nucleosynthetic W isotope variations.

To further test if this correction for nucleosynthetic anomalies based on W isotope data for bulk CAI is valid, we applied the same correction procedure to the initial $\epsilon^{182}\text{W}$ obtained from an internal Hf–W isochron for CAI. Burkhardt et al. (2008) originally reported an initial $\epsilon^{182}\text{W}$ of -3.28 ± 0.12 for the CAI isochron, which was obtained by using the $^{182}\text{W}/^{184}\text{W}$ ratios normalized to $^{186}\text{W}/^{183}\text{W}$. However, since nucleosynthetic W isotope anomalies result in different calculated initial $\epsilon^{182}\text{W}$ for different normalization procedures, the initial $\epsilon^{182}\text{W}$ of the CAI isochron was re-calculated from the data in Burkhardt

et al. (2008) using two different normalization schemes. For $^{182}\text{W}/^{184}\text{W}$ ratios normalized to $^{186}\text{W}/^{184}\text{W}$, an initial $^{182}\text{Hf}/^{180}\text{Hf}$ of $(9.81 \pm 0.41) \times 10^{-5}$ and an initial $\epsilon^{182}\text{W}$ of -3.25 ± 0.11 is obtained, whereas using $^{182}\text{W}/^{183}\text{W}$ ratios normalized to $^{186}\text{W}/^{183}\text{W}$ results in an initial $^{182}\text{Hf}/^{180}\text{Hf}$ of $(9.85 \pm 0.40) \times 10^{-5}$ and an initial $\epsilon^{182}\text{W}$ of -3.39 ± 0.13 . The newly calculated initial $^{182}\text{Hf}/^{180}\text{Hf}$ ratios are identical to the $^{182}\text{Hf}/^{180}\text{Hf} = (9.72 \pm 0.44) \times 10^{-5}$ originally reported by Burkhardt et al. (2008), because nucleosynthetic W isotope anomalies result in parallel shifts of the isochron. The newly calculated initial $\epsilon^{182}\text{W}$ are different for the different normalization procedures, however. Correcting these initials for nucleosynthetic effects using the average $\epsilon^{183}\text{W}$ of the CAI used in the isochron regression ($+0.18 \pm 0.13$) and the Arlandini slope moves the initial $\epsilon^{182}\text{W}$ from -3.25 ± 0.11 to -3.55 ± 0.25 (the uncertainty on this value includes an assumed 20% uncertainty on the slope of the $\epsilon^{182}\text{W}-\epsilon^{183}\text{W}$ correlation). Likewise, the $\epsilon^{184}\text{W}$ of these CAI is -0.11 ± 0.08 , which requires a downward correction of the initial $\epsilon^{182}\text{W}$ of -3.39 ± 0.13 to -3.45 ± 0.15 . The two corrected initial $\epsilon^{182}\text{W}$ values of -3.55 ± 0.25 (rel. $^{186}\text{W}/^{184}\text{W}$) and -3.45 ± 0.15 (rel. $^{186}\text{W}/^{183}\text{W}$) are consistent with the values derived from the W isotope data for bulk CAI (-3.61 ± 0.20 rel. $^{186}\text{W}/^{184}\text{W}$ and -3.57 ± 0.14 rel. $^{186}\text{W}/^{183}\text{W}$).

The corrected $\epsilon^{182}\text{W}$ values obtained from W isotope data normalized to $^{186}\text{W}/^{183}\text{W}$ are generally the most precise, because for this normalization nucleosynthetic anomalies on ^{182}W are the smallest, resulting in only small corrections. The weighted average of the two initial $\epsilon^{182}\text{W}$ of CAI obtained for the $^{186}\text{W}/^{183}\text{W}$ normalization ($\epsilon^{182}\text{W} = -3.57 \pm 0.14$ and $\epsilon^{182}\text{W} = -3.45 \pm 0.14$) is -3.51 ± 0.10 (2σ), which we consider the current best value for the initial W isotope composition of the solar system. This value should be used in all chronological studies.

5. CHRONOLOGY OF CORE FORMATION IN PLANETESIMALS

The downward revision of the initial $\epsilon^{182}\text{W}$ of CAI from -3.28 ± 0.12 to -3.51 ± 0.10 has important implications for the Hf–W chronometry of iron meteorites. The W isotopic composition of iron meteorites has been modified by cosmic-ray-induced neutron capture reactions, but even after correcting these effects using exposure ages and concentrations of cosmogenic noble gases (Markowski et al. 2006a; Qin et al. 2008a), many iron meteorites still have $\epsilon^{182}\text{W}$ values below the previously used CAI initial of $\epsilon^{182}\text{W} = -3.28$. This resulted in negative model ages for the irons (see Figure 7 in Burkhardt et al. 2008), which was thought to reflect an insufficient correction of the cosmic-ray effects, because neither the exposure ages nor the concentrations of cosmogenic noble gases provide a direct neutron dose monitor. Relative to the revised initial $\epsilon^{182}\text{W}$ of CAI of -3.51 ± 0.10 , however, most iron meteorites exhibit $\epsilon^{182}\text{W}$ values (corrected for cosmic-ray effects) that are identical to or slightly higher than the CAI initial (Figure 4).

The downward revision of the initial $\epsilon^{182}\text{W}$ of CAI from -3.28 to -3.51 results in Hf–W model ages for iron meteorites that are ~ 2 Myr younger. The revised Hf–W model ages indicate that core formation in most parent bodies of magmatic iron meteorites occurred within the first ~ 2 Myr after CAI formation (Figure 4), consistent with ^{26}Al being the dominant heat source causing the differentiation of early-accreted planetesimals (e.g., Hevey & Sanders 2006; Kleine & Rudge 2011; Dauphas & Chaussidon 2011). We conclude that unlike the mostly negative

model ages obtained relative to the previously used initial $\epsilon^{182}\text{W}$ of CAI, the revised Hf–W model ages for iron meteorites are positive (albeit indistinguishable from the formation of CAI), consistent with the fact that CAI are the first solids formed in the solar nebula.

The uncertainty on the revised initial $\epsilon^{182}\text{W}$ of CAI remains a major source of uncertainty when calculating Hf–W ages relative to the formation of CAI. Clearly, more high-precision W isotope data for CAI are needed to more tightly constrain the initial $\epsilon^{182}\text{W}$ of CAI. However, as demonstrated in this study, the new Hf–W data must be accompanied by high-precision measurements of non-radiogenic W isotopes, to fully quantify the contribution of nucleosynthetic isotope anomalies to variations in $\epsilon^{182}\text{W}$.

This work was supported by the Swiss National Science Foundation (No. 2-77213-08). We thank the Field Museum Chicago for generously providing the Murchison sample. The constructive review by an anonymous referee is gratefully acknowledged.

REFERENCES

- Amelin, Y., Kaltenbach, A., Iizuka, T., et al. 2010, *Earth Planet. Sci. Lett.*, **300**, 343
- Arlandini, C., Käppeler, F., & Wisshak, K. 1999, *ApJ*, **525**, 886
- Ávila, J. N., Lugaro, M., Ireland, T. R., et al. 2012, *ApJ*, **744**, 49
- Bao, Z. Y., Beer, H., Käppeler, F., et al. 2000, *At. Data Nucl. Data Tables*, **76**, 70
- Birck, J. L. 2004, in *Geochemistry of Non-traditional Stable Isotopes, An Overview of Isotopic Anomalies in Extraterrestrial Materials and Their Nucleosynthetic Heritage*, ed. C. M. Johnson, B. L. Beard, & F. Albarede (Washington, DC: The Mineralogical Society of America), 25
- Bouvier, A., & Wadhwa, M. 2010, *Nat. Geosci.*, **3**, 637
- Burkhardt, C., Kleine, T., Dauphas, N., & Wieler, R. 2012, in *Proc. 43rd Lunar and Planetary Sci. Conf. (LPI Contribution No. 1659; Houston, TX: LPI)*, 2405
- Burkhardt, C., Kleine, T., Oberli, F., et al. 2011, *Earth Planet. Sci. Lett.*, **312**, 390
- Burkhardt, C., Kleine, T., Palme, H., et al. 2008, *Geochim. Cosmochim. Acta*, **72**, 6177
- Dauphas, N., & Chaussidon, M. 2011, *Annu. Rev. Earth Planet. Sci.*, **39**, 351
- Grossman, L. 1972, *Geochim. Cosmochim. Acta*, **36**, 597
- Harper, C. L., & Jacobsen, S. B. 1996, *Geochim. Cosmochim. Acta*, **60**, 1131
- Hevey, P. J., & Sanders, I. S. 2006, *Meteor. Planet. Sci.*, **41**, 95
- Humayun, M., Simon, S. B., & Grossman, L. 2007, *Geochim. Cosmochim. Acta*, **71**, 4609
- Jacobsen, S. B. 2005, *Annu. Rev. Earth Planet. Sci.*, **33**, 531
- Kleine, T., Hans, U., Irving, A. J., & Bourdon, B. 2012, *Geochim. Cosmochim. Acta*, **84**, 186
- Kleine, T., Mezger, K., Münker, C., Palme, H., & Bischoff, A. 2004, *Geochim. Cosmochim. Acta*, **68**, 2935
- Kleine, T., Mezger, K., Palme, H., Scherer, E., & Münker, C. 2005, *Geochim. Cosmochim. Acta*, **69**, 5805
- Kleine, T., Münker, C., Mezger, K., & Palme, H. 2002, *Nature*, **418**, 952
- Kleine, T., & Rudge, J. F. 2011, *Elements*, **7**, 41
- Kleine, T., Touboul, M., Bourdon, B., et al. 2009, *Geochim. Cosmochim. Acta*, **73**, 5150
- Lee, D. C., & Halliday, A. N. 1995, *Nature*, **378**, 771
- Leya, I., Wieler, R., & Halliday, A. N. 2003, *Geochim. Cosmochim. Acta*, **67**, 529
- Ludwig, K. 1991, U.S.G.S. Open File Report 91-0445
- Markowski, A., Leya, I., Quitté, G., et al. 2006a, *Earth Planet. Sci. Lett.*, **250**, 104
- Markowski, A., Quitté, G., Halliday, A. N., & Kleine, T. 2006b, *Earth Planet. Sci. Lett.*, **242**, 1
- Masarik, J. 1997, *Earth Planet. Sci. Lett.*, **152**, 181
- Nyquist, L. E., Kleine, T., Shih, C. Y., & Reese, Y. 2009, *Geochim. Cosmochim. Acta*, **73**, 5115
- Qin, L. P., Dauphas, N., Wadhwa, M., Masarik, J., & Janney, P. E. 2008a, *Earth Planet. Sci. Lett.*, **273**, 94
- Qin, L. P., Dauphas, N., Wadhwa, M., et al. 2008b, *ApJ*, **674**, 1234
- Reisberg, L., Dauphas, N., Luguét, A., et al. 2009, *Earth Planet. Sci. Lett.*, **277**, 334
- Scherstén, A., Elliott, T., Hawkesworth, C., Russell, S. S., & Masarik, J. 2006, *Earth Planet. Sci. Lett.*, **241**, 530
- Schoenberg, R., Kamber, B. S., Collerson, K. D., & Eugster, O. 2002, *Geochim. Cosmochim. Acta*, **66**, 3151
- Scott, E. R. D., & Wasson, J. T. 1975, *Rev. Geophys.*, **13**, 527
- Wasserburg, G. J., Wimpenny, J., & Yin, Q.-Z. 2011, in *Proc. Workshop on Formation of the First Solids in the Solar System (LPI Contribution No. 1639; Houston, TX: LPI)*, 9038
- Yin, Q. Z., Jacobsen, S. B., Yamashita, K., et al. 2002, *Nature*, **418**, 949